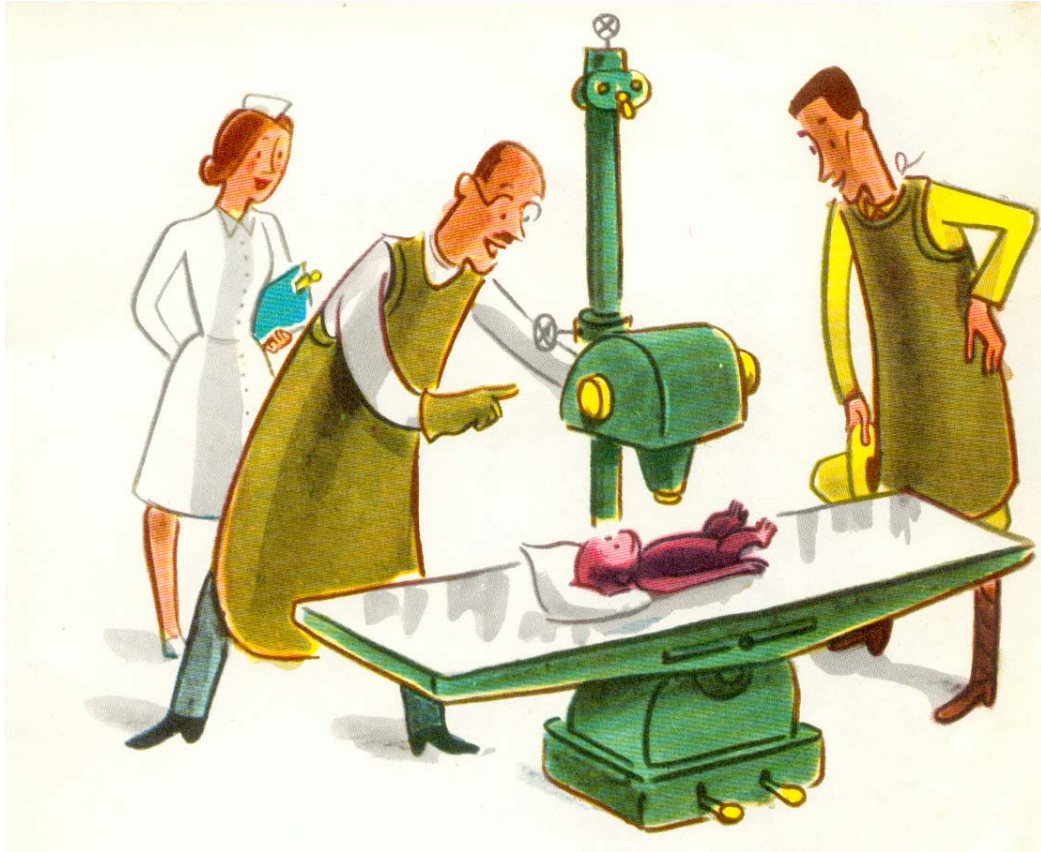


CT



AK, EF, MCT & IV

Computed Tomography
lab instructions
January 2013
KTH STH

Please read these instructions carefully before you take part in the laboratory exercise. If there are parts that you don't understand you can ask the lab assistant or MCT; You don't need to know everything in detail but should have a general understanding of the material.

It is compulsory to solve the preparatory exercises on page 19 (preferably not in group) and to write down the solution. Do ask MCT for help before the lab-day if you get stuck!

Please note that if you do not have (at least an attempt to) a solution to the preparatory exercises to show to your lab-assistant at the beginning of the lab-session you will be denied to participate in the lab-exercise.

Contents

Introduction	2
Interaction of X-rays with matter	3
Absorption of X-rays in matter	5
The principles of computed tomography	8
The mathematics of CT	8
Image reconstruction	9
The KTH-STH CT set up	12
The X-ray source	12
The X-ray detector	13
Laboratory exercise	18
Preparatory exercises	19
The report	20

Introduction

X-rays were discovered (accidentally) by a German physicist, Wilhelm Konrad Röntgen in 1895. A few years later, in 1901, Röntgen was awarded the first Nobel Prize in physics for his discovery, and since then, X-ray imaging has been the most important and most widely used tool in clinical medicine. The technique of traditional X-ray imaging of today does not differ much from Röntgen's. An object is irradiated by photons from an X-ray source and the transmitted photons are registered on a x-ray detector. Since X-ray attenuation in tissue is proportional to electron density, the X-ray intensity that traversed a region of lower density (e.g. muscle) will be greater than what has traversed a region of higher density (e.g. bone). In other words, the gray scale of the image is inversely proportional to the attenuation of the tissue in the ray path.

Despite being the most commonly used clinical method, X-ray imaging does have some serious drawbacks. The 2-dimensional image will be a complex superposition of all the structures of the 3-dimensional body; the depth information is lost. Furthermore, the size on the image of an object is dependent on its distance to the X-ray source resulting in a distorted scaling factor of the picture. In addition, as will be explained in

the next section, the contrast of the image suffers from limited dynamic range of the attenuation coefficients in the human body. All these obstacles found their solutions in Computed Tomography, CT.

During the last decade the use of CT has increased dramatically as a diagnostic tool in hospitals, but the idea is not new, and the mathematical basis was developed already in 1917 by the Austrian mathematician Johann Radon [1]. Radon was working on gravitational waves, but the plan to use his math to do 3-dimensional X-ray imaging was dwelling under the surface up to the 1960's when there was enough computer power to make reconstruction realizable. In the early 1960's, Allan Cormack from Tufts University published his work on CT as a new approach for imaging [2, 3], and the first scanner was built by Godfrey N. Hounsfield at EMI in England in 1972 [4]. Cormack and Hounsfield were awarded the Nobel Prize in Physiology and Medicine in 1979.

To demonstrate the principles of CT, a set-up for educational purposes has been designed and constructed. The system is much simpler than a clinical CT scanner, but the aim is the general understanding of the principles of CT, the data acquisition, and the image reconstruction process.

Interaction of X-rays with matter

X-rays used for clinical radiology are so called hard X-rays with a wavelength in the region around 0.1-0.01 nm, as opposed to soft X-rays with a longer wavelength. Electromagnetic waves with a shorter wavelength are usually referred to as gamma rays. The distinction between gamma and X-rays in terms of energy or wavelength is not precisely defined, though, and often electromagnetic radiation is referred to as X-ray or gamma depending on the way it is produced instead. Since the energy of x- and gamma radiation is so high, the radiation is quantized and can be regarded as a stream of single photons. Therefore, instead of the wavelength, the energy of each photon is most often used to characterize the radiation, which is related to the wavelength according to $E = hc/\lambda$, where h is Planck's constant. The energy interval of diagnostic X-rays is approximately 10–200 keV.

X- and gamma radiation experience mainly three different types of basic interactions in matter, namely photoelectric effect, Compton scattering, and pair production. The type of process that dominates depends on the energy of the radiation; at low energies the photoelectric effect dominates, while at intermediate energies the Compton scattering is the most important, and finally at high energies the pair production mechanism will dominate. For diagnostic X-rays, the dominant processes are the photoelectric effect and Compton scattering. A fourth type of interaction which has some influence, but is never dominating in the X-ray region, is Rayleigh scattering.

Photoelectric effect

The photoelectric effect (PE) is the complete absorption of an incoming photon upon interaction with an atomic electron. All the energy of the photon is transferred to the electron, which is emitted from the atom with an energy T_e given by:

$$T_e = E_\gamma - E_b$$

where E_γ is the energy of the photon, and E_b is the atomic binding energy of the electron. From this relation it is obvious that a requirement for the PE to be possible is that the photon energy exceeds the atomic binding energy of the electron.

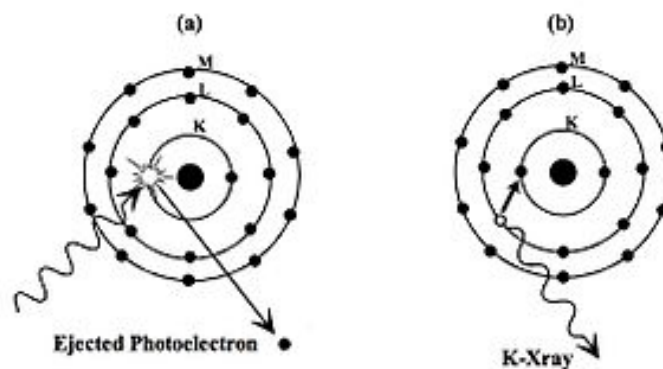


Figure 1: *The Photoelectric Effect - (a) photon absorption and electron ejection and (b) fluorescent X-ray emission. (image from the wikibook Basic Physics of Digital Radiography by Kieran Maher*

For reasons that are difficult to explain in this brief paper and that are outside the scope of this course the probability for PE is at a maximum when the energy of the incoming photon is just that of the binding energy of the electron (in any given shell) and reduces approximately with the cubed root of the photon energy, E_γ . The interaction probability is greater the more tightly bound the electron is, implying that PE is more probable for atoms with large atomic numbers and for the inner shells in the atom. This probability is very approximately proportional to the cube of the atomic number, Z . Considering the two factors above, one can say that the probability for PE is roughly proportional to $\frac{Z^3}{E_\gamma^3}$ with sharp edges corresponding to the binding energy of each shell.

Fig. 3 can be interpreted very easily by keeping in mind what stated above.

Compton and Rayleigh scattering

Compton scattering is the scattering of photons by free electrons. There are of course no free electrons in matter, but if the photon energy is large compared to the binding

energy of the electron, the electron can be considered as free to a good approximation. The photon is not absorbed as in PE and continues after some loss of energy and a change of direction. The kinematics of the interaction is illustrated in fig. 2.

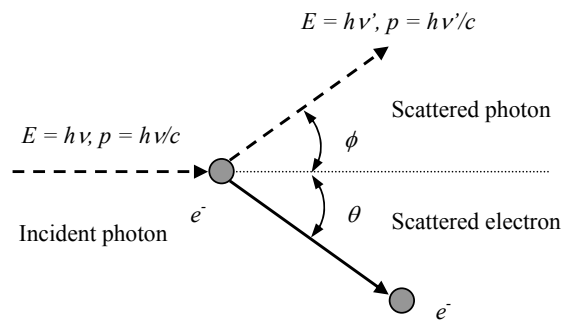


Figure 2: Kinematics of Compton scattering

Applying the conditions of conservation of energy and momentum it is possible to show that the energy of the scattered photon as a function of the scattering angle and of the energy of the incident photon will be:

$$h\nu' = \frac{h\nu}{1 + \frac{h\nu}{m_e c^2 (1 - \cos \phi)}}$$

Rayleigh scattering is the scattering of a photon by an atom. There is basically no energy loss, and the directional change is also much smaller than that for Compton scattering.

Pair production

This interaction process only occurs at energies above 1,022 MeV and is thus irrelevant for medical X-ray imaging. It is an interesting process though; ask your lab assistant if you want more information!

Absorption of X-rays in matter

As a result of the interactions described above the photons are either scattered with some loss of energy, or completely absorbed in a photoelectric interaction. This means that photons will disappear from the beam as a result of interactions. Only those photons that have not undergone any interactions at all remain in the (well-collimated) beam, which means that a beam of photons is not degraded in energy as a result of passing through matter, just attenuated in intensity (number of photons per unit time and unit area).

The probability of photon attenuation can be expressed as a function of the thickness of the attenuator, the Beer law

$$I(x) = I_0 e^{-\mu x} \quad (1)$$

where the linear attenuation coefficient μ has units of [1/length], for instance [cm^{-1}]. In other words, Eq. 1 says that the linear attenuation coefficient μ is the fractional change in intensity of the incident beam per unit thickness of the attenuating material. The linear attenuation coefficient is a function of both the energy of the photons and the elemental composition of the attenuating material. This is a fact that medical imaging with photons relies on.

The linear attenuation coefficient depends on the density, ρ , of the absorbing material. This dependency can be overcome by normalizing the linear attenuation coefficient for density, and the normalized term is called the mass attenuation coefficient, μ_ρ :

$$\mu_\rho \equiv \frac{\mu}{\rho}$$

Simple dimensional analysis gives units [length²/mass] for the mass absorption coefficient. Usually μ_ρ is given in cm^2/g .

Mass attenuation coefficients for various materials of interest for medical imaging are presented on the webpage of the National Institute for Standards and Technology (NIST)¹. The density of the various materials is also presented so that the linear attenuation coefficient can be found. The mass attenuation coefficient as function of photon energy is displayed for aluminum and lead in Fig. 3.

Some linear attenuation coefficients at a 30 keV X-ray beam are:

$$\begin{aligned} \mu_{\text{air}} &\approx 0 \text{ cm}^{-1} \\ \mu_{\text{bone}} &= 2,6 \text{ cm}^{-1} \\ \mu_{\text{muscle}} &= 0,40 \text{ cm}^{-1} \\ \mu_{\text{blood}} &= 0,41 \text{ cm}^{-1} \end{aligned}$$

Evidently, the differences are very small for soft tissue (muscle and blood), and since X-ray films usually have a contrast limit of 2%, soft tissue structures are hardly detected in traditional X-ray imaging. This can be illustrated by the following calculation:

A 1 cm rib and a 1 cm air-filled volume in the lung are easily distinguishable:

$$C = \frac{I_{\text{air}} - I_{\text{bone}}}{I_{\text{air}}} \Rightarrow C = 1 - \frac{e^{-2,6 \cdot 1}}{e^{-0,1}} = 0,93 \Rightarrow 93\% \text{ contrast,}$$

¹ <http://www.physics.nist.gov/PhysRefData/XrayMassCoef/cover.html>.

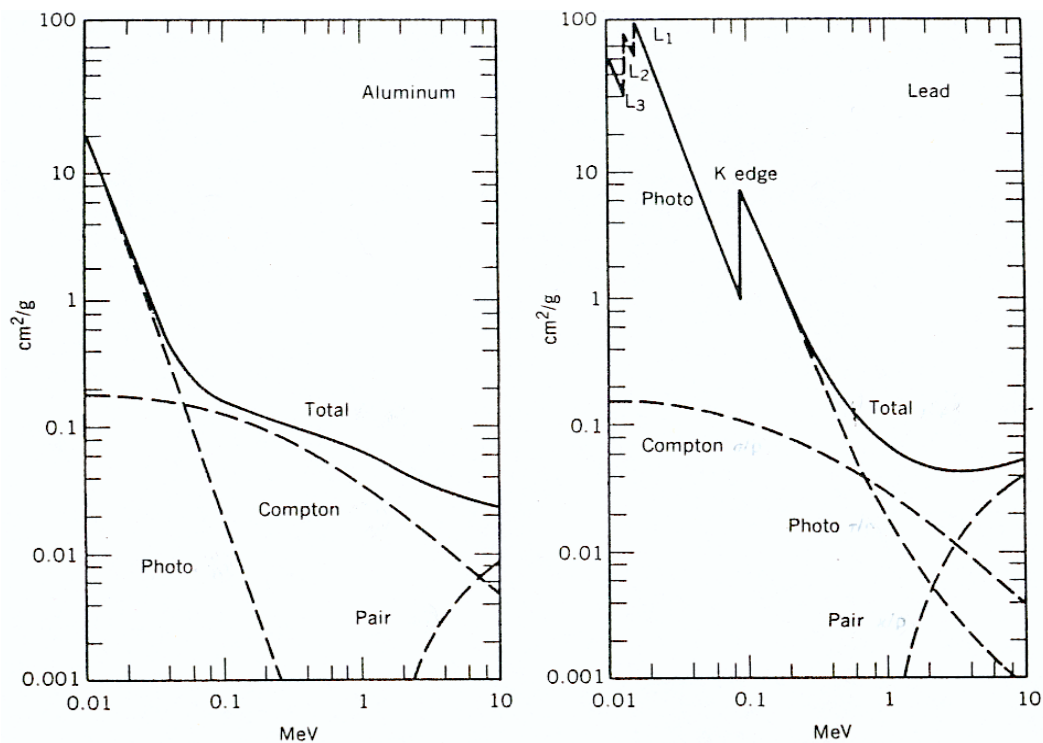


Figure 3: Mass absorption coefficient for aluminum and lead for the three individual processes involved (Photo, Compton and pair production) and the sum of the three components as a function of the photon energy. Note the presence of the K and L edges reflecting the binding energy of the electron in the material. These edges are not visible for Al due to their low energies.

while a blood filled vessel of the same dimension embedded in muscle is not visible:

$$C = \frac{I_{\text{muscle}} - I_{\text{blood}}}{I_{\text{muscle}}} \Rightarrow C = 1 - \frac{e^{-0,41 \cdot 1}}{e^{-0,40 \cdot 1}} = 0,01 \Rightarrow 1\% \text{ contrast.}$$

Additionally, this calculation does not take into account the superposition of tissue structures above and below the area of interest, which deteriorates the contrast even further.

One way to overcome the low contrast is to use liquid contrast media with a high attenuation coefficient, for instance iodine compounds, which can be injected into the vascular system of the patient. The atomic number of iodine is 54 compared to the main constituents of soft tissue: 1 for hydrogen, 8 for oxygen, and 6 for carbon. Another way to detect the soft anatomy of the human body is by using CT. CT is able to present images from structures with extremely small differences in linear attenuation coefficient, e.g. observing a tumor surrounded by soft tissue. This is partly due to the

use of digital detectors with the ability to show much smaller contrast differences. The main reason is, however, the elimination of under- and overlying tissue structures.

The principles of computed tomography

The first CT scanners to appear were the so called first generation scanners. They are conceptually simple and later generation CT scanners are build on the same principles. A planar slice of the body is examined by measuring the attenuation of a narrow beam (pencil beam) of X-rays for different positions and directions (Fig. 4). The pencil beam passes through the object and is detected on the far side, and the source-detector assembly is scanned sideways to generate one projection (a set of attenuation data for one angle). This is repeated for many angles to obtain a set of projection data.

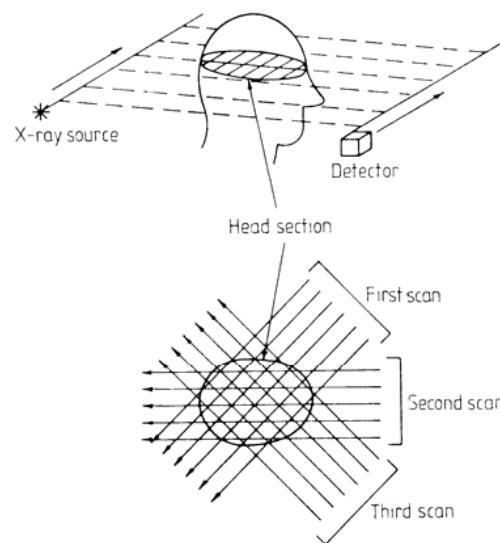


Figure 4: *The principle of the first generation CT scanners.*

The mathematics of CT

Two different coordinate systems have to be defined (see Fig. 5), one that is fixed in the object, (x, y) , and another one that rotates with the source and detector, (x', y') . The sought two-dimensional distribution is that of the linear attenuation coefficient $\mu(x, y)$. $F_\phi(x')$ is the projection for a certain angle, ϕ , which is obtained by moving the X-ray source and the detector along the x' axis.

The attenuation of an X-ray beam along a straight line AB through the object is a function of the y' coordinate, and each infinitesimal element dy' gives a contribution to the total attenuation. Each data point in a projection is a measure of the total attenuation of the X-ray beam, which is the sum of all those infinitesimal contributions and hence a line integral along AB. This means that if the following assumptions are made:

- i) the X-ray beam is a narrow pencil beam;
- ii) the radiation is monoenergetic;
- iii) no scattered radiation hits the detector;

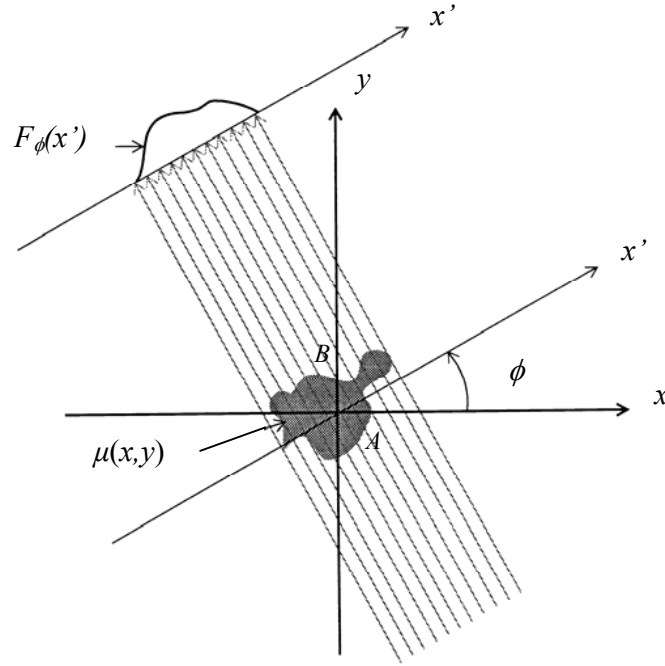


Figure 5: The coordinate systems in CT. The function $F_{\phi}(x')$ is the Radon transform of $\mu(x, y)$ for the angle ϕ .

then the transmitted X-ray intensity along the line AB is given by the expression:

$$I_{\phi}(x') = I_{\phi}^0(x') e^{-\int_{AB} \mu(x, y) dy'} \quad (2)$$

where AB is a straight line parallel to the y' axis located at the distance x' from the origin, and ϕ is the angle between the (x, y) and (x', y') frames. From this expression the projection of the object measured at an angle ϕ and distance x' is defined by the *Radon transform*:

$$F_{\phi}(x') = -\ln \left(\frac{I_{\phi}(x')}{I_{\phi}^0(x')} \right) = \int_{-\infty}^{\infty} \int_{-\infty}^{\infty} \mu(x, y) \delta(x \cos \phi + y \sin \phi - x') dx dy \quad (3)$$

Since the equation of the straight line AB is $x' = x \cos \phi + y \sin \phi$, the Dirac delta function makes sure that the integration is carried out only along the line AB.

Image reconstruction

To calculate the image, which is the same as the function $\mu(x, y)$, the Radon transform (Eq. 3) must be inverted using an *inverse Radon transform*. This operation is called *image reconstruction* and it is not a trivial task with a general solution. The simplest

way of image reconstruction is the *back-projection method* and its principles are shown in Figs. 6 and 7. The projection at a given angle is an array of attenuation values. These values are "smeared out" evenly along the projection line, and the process is repeated for all angles to create an image matrix. The quality of the reconstructed image is improved with increasing number of projections.

The back-projection method relies on the Fourier slice theorem, which in effect states that it is possible to reconstruct an object from a set of projections provided that the projection data set contains enough information. By enough information is meant that the projections must be taken for a large number of angles over a complete half revolution (180°). This method involves Fourier transformation of the data set with respect to spatial coordinates (x' and ϕ).

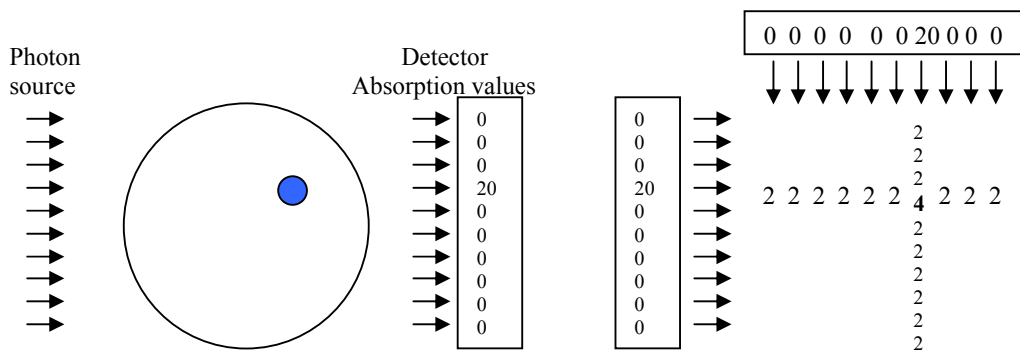


Figure 6: *Recording of a projection ... and back-projection of recorded data.*

A star-shaped pattern appears around each dense object when using the simple back-projection method, as can be seen in Fig. 7. Statistical fluctuations are usually also present in any data set. After Fourier transformation of the data these fluctuations appear as high-frequency noise in the spatial frequency domain. One drawback of the back-projection method is that such high-frequency components are amplified unproportionally. By applying appropriate filters, however, artefacts and noise can be suppressed. Therefore, the most commonly applied method is the so called *filtered back-projection algorithm*. A filter is a mathematical function that the data is multiplied by in

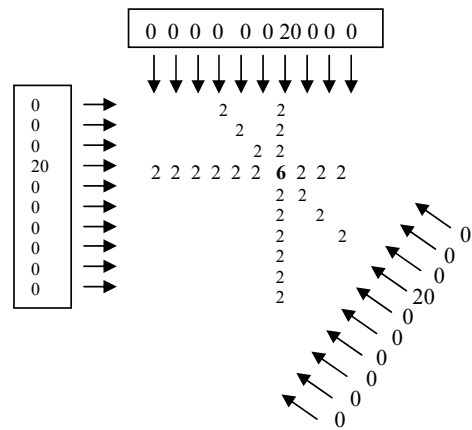


Figure 7: *Back-projection of data from three directions.*

the process of transformation. Commonly used filters are for instance Ramachandran-Lakshminarayanan, Shepp-Logan, Hamming, Hann, and Butterworth filters.

From narrow pencil beam to fan beam geometry

The CT-demonstrator used in this laboratory exercise has a more modern design than the first generation CT scanners presented in the previous section. The main difference is that the X-ray source does not produce a pencil beam but a *fan beam* of X-rays (third generation CT). In this way a projection of the object can be obtained in one go, without any need of translating the source as in the narrow pencil beam case.

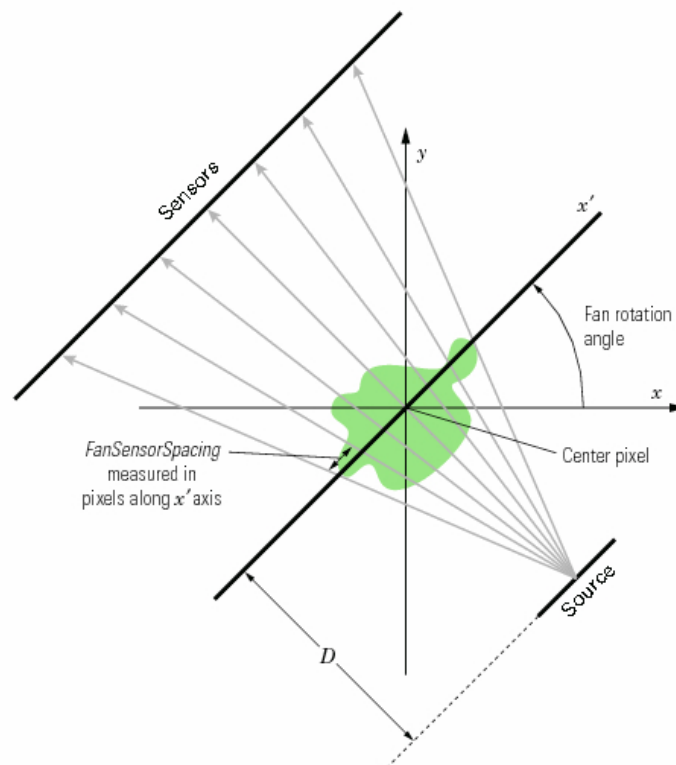


Figure 8: *Fan beam projection (figure from the MATLAB user manual).*

Data obtained with a fan-beam source (see Fig. 8) can be transformed to parallel beam projection data (as in Fig. 5) before proceeding to image reconstruction. The procedure is described in details in Chapter 3 of the book by A. C. Kak & M. Slaney [5] (freely available from <http://www.slaney.org/pct/pct-toc.html>).

From translate-rotate to helix

The first generation CT scanners used a translate-rotate movement in order to scan the object *slice by slice*. Our demonstrator instead can be used in two other ways: Data can be collected slice by slice by translating the object after recording a 2D-slice (translate-rotate) or, for faster acquisition, the object can be rotated and translated at the same time. This second method is the so called *helix CT* geometry that is commonly used in modern clinical scanners. The only difference is that in the KTH STH demonstrator it is the object that rotates and not the source and detector. The helix CT geometry allows a much shorter scanning time and avoids the stress on the gantry, tube and detectors that stopping and starting (accelerating) brings on. It requires though an extra step in the reconstruction stage in order to *re-assemble* the object (see Fig. 9).

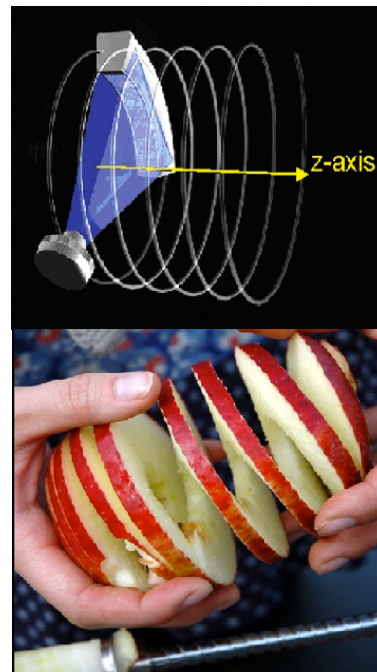


Figure 9: *Scanning with the helix CT geometry.*

The KTH-STH CT set up

The X-ray source



Figure 10: *Mini-X X-ray tube (figure from the Amptek website).*

The X-ray source in our set up is the USB-controlled *mini-X X-ray tube* by Amptek,

Inc. with a silver target (0,75 μm thickness) with a focal spot size of approximately 2 mm. The tube works in the voltage range 10 – 50 kV (while only a 12 V input voltage is supplied through the USB) and in a current range 5 – 200 μA , with a maximum continuous power of 4 W.

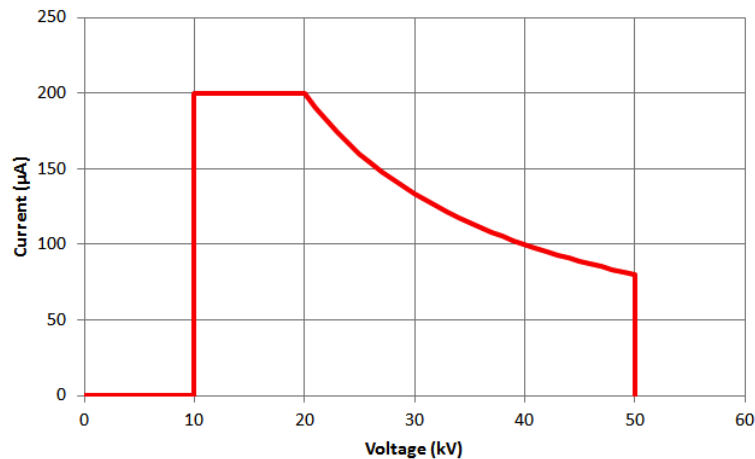


Figure 11: *Mini-X isopower curve (figure from the Amptek website).*

127 μm thick Beryllium is used as window material. The flux is approximately 10^6 photons/(s·mm²) at a distance of 30 cm when the tube is operated @50 kV/1 μA . The output cone angle is 120° but it can be collimated to a pencil beam of 1 mm by means of a brass collimator.

The spectrum of the tube at 50 kV is shown in Fig. 12. The K_α and K_β edges are clearly visible.

The X-ray detector

The detector is a line detector constituted by three main blocks:

1. Hamamatsu S8865-128G: This is a photodiode array with an amplifier and a phosphor sheet attached to the photosensitive area for X-ray detection
2. Hamamatsu C9118 driver circuit: CMOS driver circuit generating a timing signal and serving as a video signal processor
3. ATOMKI mini2440: DAQ board designed and constructed at ATOMKI by the marvelous Iván Valastyán

Let's see how they work in principle

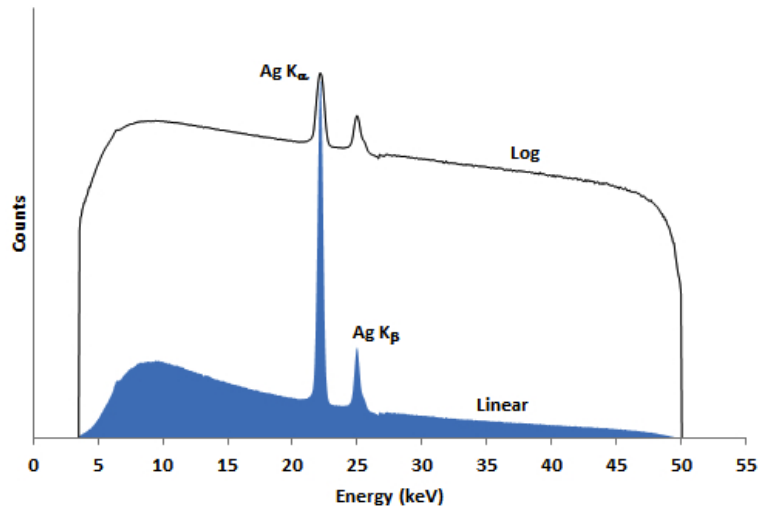


Figure 12: *Mini-X Silver (Ag) X-ray tube output spectrum (figure from the Amptek website).*

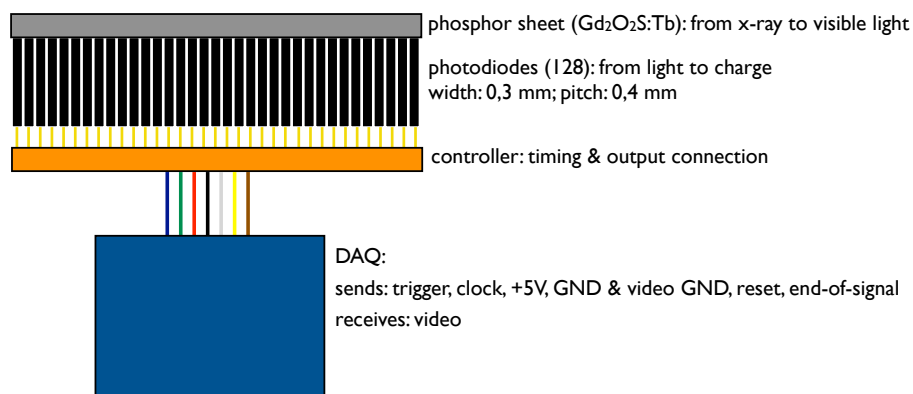


Figure 13: *Conceptual scheme of the detector.*

Hamamatsu S8865-128G+Hamamatsu C9118 driver circuit

When an X-ray interacts with the $300\ \mu\text{m}$ phosphor (scintillator), $\text{Gd}_2\text{O}_2\text{S:Tb}$, a number of visible photons are created. These photons will then create charge in the elements of the photodiode array that are nearby the point of interaction. Actually, since the thickness of the phosphor is only $300\ \mu\text{m}$, the most likely outcome is that only one photodiode is fired per X-ray).

The charge generated by one single X-ray is too small to be used as a signal as it would be drowned in the dark current of the device. For this reason the charge is read after a certain interval of time (integration time) that can be adjusted through the controller. If you remember what you have learned in the detector laboratory, this means that the

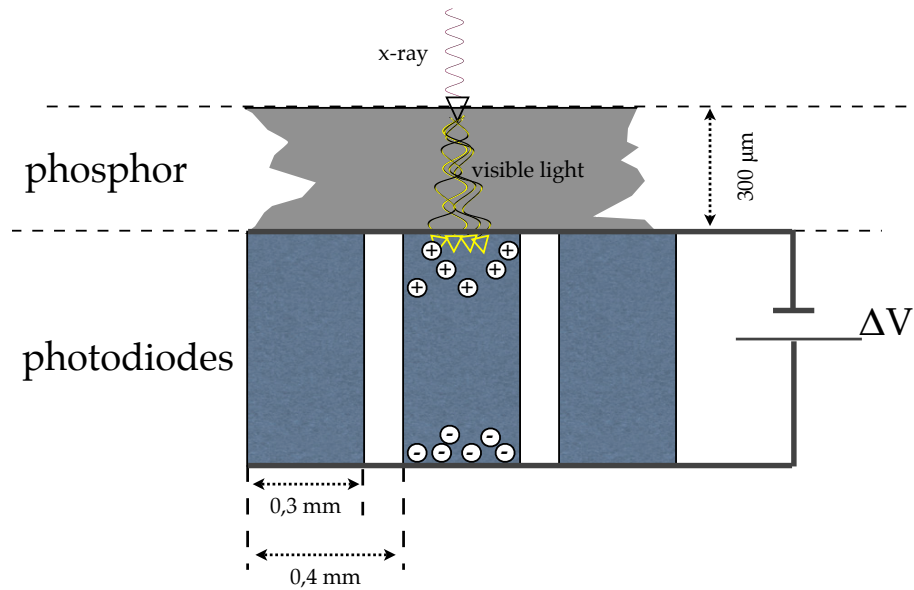


Figure 14: Working principle of the photodiode array + phosphor.

detector is working in current mode. After the integration time the signal from each of the 128 pixels (a 2 byte unsigned integer with values from 0-1023) is acquired giving a total of 256 bytes for each TCP/IP packet and each of the pixels is reset in order to start a new acquisition. During the reset time the detector is not able to collect any data (dead time).

The detector line is 51,2 mm wide giving a pixel size of 0,4 mm in this direction. The height of the $Gd_2O_2S:Tb$ sheet is 0,6 mm.

DAQ: ATOMKI mini2440

The mini2440 is an ARM9 processor (405 MHz) based Single Board Computer (SBC). Besides the conventional computer interfaces (e.g. audio, Ethernet, USB, serial) it is equipped with special interfaces, such as 8-channel 10-bits analog to digital converter, a GPIO (general purpose input output) interface, an I2C bus and 4 pulse-width modulation (PWM) units.

The board runs embedded Linux from a built-in flash memory. Fig. 15 shows the mini2440 board. The detector is connected to the input output connector located in top-left corner.

In order to provide the control signals (clock and reset) required by the Hamamatsu pixel-array detector a dedicated software is running on the board which controls the PWM outputs and samples the ADC channels to acquire video, trigger and end of signals pulses. The board also provide the GND and +5V for the detector array.

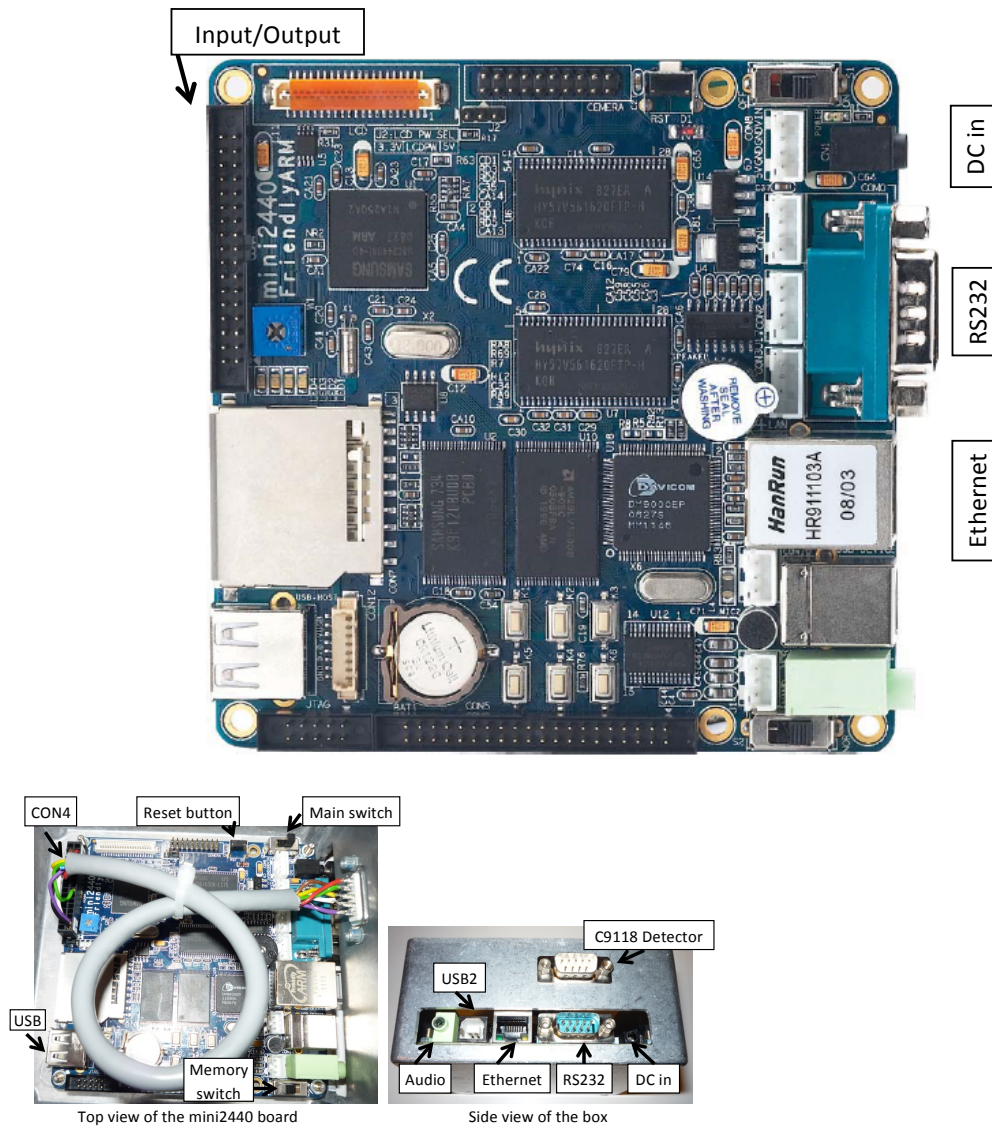


Figure 15: The mini2440 board (upper). Top and side view of the mini2440 as mounted in the KTH Helix CT (lower)

The embedded control program also processes the video signals of the pixels and sends them to the PC via standard Ethernet protocol.

Monitoring of the Linux console is made possible through the serial interface (RS232-connection) using a hyperterminal.

The acquisition program, running on the PC, controls the mini2440 board receives and stores data.

Basic geometrical parameters

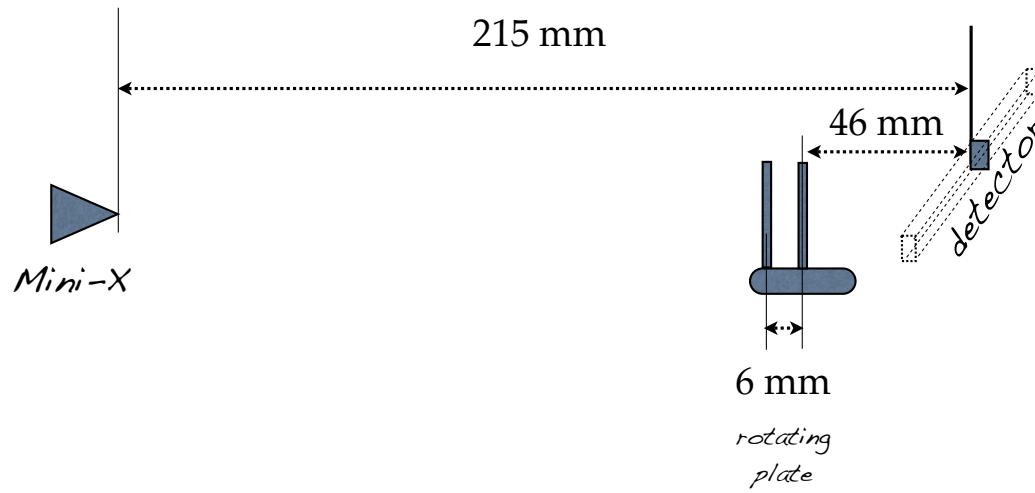


Figure 16: Geometrical parameters of the CT scanner

Laboratory exercise

Caution

The Mini-X contains a high voltage power supply. The high voltage power supply has been thoroughly tested and should not ever arc to its own case. However, if at any time any high voltage arcing or popping is heard, immediately discontinue use. High voltage arcing has a distinctive sharp cracking sound. The Mini-X produces X-RAYS when energised. Never open the shielding box while the Mini-X is being energised and never put your hands, your eyes or any other part of your body in front or near the Mini-X while in operation.

1. Start the ATOMKI mini2440 DAQ by switching on its power and start the hyperterminal. Start the KTH Helix CT GUI and connect to the detector
2. Without switching on the source, check the detector count rate per pixel: Why is not the count rate 0?
3. Switch on the dark current correction and check the count rate now.
4. Start the MiniX X-ray tube and set the voltage to 48 kV and the current to 78 μA (to avoid freezing: set voltage to 40 kV and current to 78 μA , then start and after few seconds update to 48 kV and click on "Set voltage and current")
5. Check the detector count rate without any object. Explain its shape and relate its amplitude to what seen in point 2.
6. Put the Fe-cylinder in the camera to check horizontal alignment. Is it OK?
7. Put now a plastic pipette in the camera. Does the detector show a reasonable shape?
8. Put now the KTH CT experimental pencil (2,2 mm diameter graphite). Is the attenuation compatible with the given dimensions of the pencil?
9. Change now the object to the plastic cylinder. Put it first in the position closer to the detector and look at the attenuation profile. Take note of the width in pixels. Rotate it now by 180° and check again the width in pixels. Does the width change? Why? Translate now the width from pixels to mm. Is the width compatible with the object?
10. Acquire data for plotting the sinogram with the plastic cylinder and the plastic parallelepiped. Then you can use the given reconstruction program to show the sinograms. What happens in you try the back-projection without filtering? (Try that by changing the filter line in the reconstruction code).
11. Take a CT scan of the beautiful doll provided. Her name is Skipper and she is in good health.

Preparatory exercises

1. Which are the three major interaction modes of photons with matter at X-ray energies important for medical imaging?
2. The probability of the three interaction processes depend on the energy of the incoming photons. Which interaction modes dominate in which energy regions?
3. As can be seen in Fig. 3, the amplitude of the attenuation coefficient exhibits drastic changes (edges) in the low energy region. These edges depend on the absorbing material. Explain!
4. In traditional X-ray examination the detection limit (i.e. the measurable intensity change) is 2%. Is it possible to observe a 1 mm diameter bone surrounded by soft tissue, for example in a human, using 20 keV or 50 keV photons? For attenuation coefficients use NIST:
<http://www.physics.nist.gov/PhysRefData/XrayMassCoef/cover.html>.
5. The X-ray tube used in this lab emits the spectrum shown in Fig. 12. The beam is then filtered with 25 μm of Cu. Estimate the shape of the spectrum after the Cu-filter.
6. Estimate the attenuation of the beam by a plastic absorber of 1 mm, 2 mm and 5 mm, respectively. Estimate even the attenuation by a 2,2 mm thick pencil lead. You will check these results during your lab.
7. Estimate the efficiency of 300 μm $\text{Gd}_2\text{O}_2\text{S:Tb}$ for detecting the X-ray of the beam.
8. Estimate the attenuation from the shielding of the KTH STH helix CT demonstrator. The shielding is made of 1 mm lead, 1 mm steel and 3 mm aluminium.
9. A plastic cylinder with diameter 8 mm is put in the middle of the rotating plate of the CT-demonstrator (see fig. 16). What is the width of the image (projection) on the detector?
10. Who is the patient on the front page of this document and what are his symptoms? Who are the people standing around him?

The report

The report should consist of the following parts:

Introduction. What are the basic principles behind CT? Why does one want to do CT instead of regular x-ray imaging? How did CT evolve? Which advantages and disadvantages of CT compared to other imaging modalities such as Magnetic Resonance Imaging (MRI) and 3D Ultrasound can you find? Please do not just copy the lab instructions, but include information from elsewhere; the lab assistant will give you more information than is in the instructions, and there are tons of information easily accessible on the internet.

Materials and methods. This is where you describe the KTH-CT set-up. What are the different parts, what are their respective functions, and how are they connected? How does the data acquisition work and how is the image reconstruction implemented? Describe in particular how the sinogram is formed and its meaning.

Results. Put all the images and plots in this section. Describe briefly how they were acquired; exposure times, number of angles and positions, interpolation and filtering methods, etc.

Discussion and conclusions. Please comment on the obtained data. Is the result good or bad? What could be improved? How is the image reconstructed? What are the differences between the CT demonstrator and a clinical CT scanner? Do you think CT will be used also in the future or do you think it will be replaced by something else?

Answers to the preparatory exercises.

Please send the report to the lab assistant within one weeks from your lab-day! Remember that it is easier to write a report soon after the exercise!

Bibliography

- [1] Johann Radon. On the determination of functions from their integral values along certain manifolds. *IEEE Transactions On Medical Imaging*, MI-5:170–176, 1986.
- [2] A.M. Cormack. Representation of a function by its line integrals, with some radiological applications. *Journal of Applied Physics*, 34(9):2722–2727, 1963.
- [3] A.M. Cormack. Representation of a function by its line integrals, with some radiological applications. ii. *Journal of Applied Physics*, 35(10):2908–2913, 1964.
- [4] G.N. Hounsfield. Computerized transverse axial scanning (tomography): Part 1. description of system. *British Journal of Radiology*, 46(552):1016–1022, 1973.
- [5] A. C. Kak and M. Slaney. *Principles of Computerized Tomographic Imaging*. Society of Industrial and Applied Mathematics, 2001.